

Leaking billiards

Jan Nagler, Moritz Krieger, Marco Linke, Johannes Schönke, and Jan Wiersig
Institut für Theoretische Physik, Universität Bremen, Otto-Hahn-Allee, D-28334 Bremen, Germany
 (Received 13 December 2006; published 10 April 2007)

Billiards are idealizations for systems where particles or waves are confined to cavities, or to other homogeneous regions. In billiard systems a point particle moves freely except for specular reflections from rigid walls. However, billiard walls are not always completely reflective and measurements inside can also open the billiard. Since boundary openings have been studied extensively in the literature, we rather model leakages inside the billiard. In particular, we investigate the classical dynamics of a leakage for a continuous family of billiard systems, that is, the stadium-lemon-billiard family. With a single parameter the geometry of the billiard can be tuned from stadium (being fully hyperbolic) over circle (integrable) to the lemon-shaped billiard (mixed chaotic). For the stadium billiard we found an algebraically decaying mean escape time with the linear size ϵ of the leakage $\langle n_{\text{esc}} \rangle \sim \epsilon^{-1}$ together with an exponential decay of the survival probability distribution. The finding is nearly independent of the position and size of the leakage, as long as the leakage is much smaller than the system size, and it is in good agreement with a stochastic map approximation of the dynamics. Due to the mixed phase space for lemon billiards, the mean escape time depends both on the position and geometry of the leakage. For systems where quasiregular motion dominates, we found a linear dependence of the mean escape time, $\langle n_{\text{esc}} \rangle \sim 1 - \epsilon$, which we refer to as *flooding law*. Our findings are helpful in understanding dynamics of leaking Hamiltonian systems.

DOI: [10.1103/PhysRevE.75.046204](https://doi.org/10.1103/PhysRevE.75.046204)

PACS number(s): 05.45.Ac, 05.45.Pq

I. INTRODUCTION

Billiard systems have been intensively studied over several decades both experimentally and theoretically. In the great majority of billiards considered in the literature a perfectly reflecting boundary encloses a domain in which the long-term dynamics of a freely moving particle or wave is under investigation. Examples for integrable (regular) billiards represent rectangular, elliptic, and circular geometries. In almost every case, the slightest deformation makes them nonintegrable. Consider, for example, the stadium billiard in Fig. 1. Whereas every starting position in phase-space of the circle billiard ($a=0$) corresponds to regular motion, for $a > 0$ the motion is ergodic, mixing, and exponentially unstable with Lyapunov exponent $\lambda \sim a^{1/2}$ for $a \ll 1$ [1].

Theory and experiments on the wave dynamics in microwave cavities and quantum dots have greatly benefited from each other with the consequence of a considerable number of publications [2–7], see Ref. [8] for an overview. Also, optical billiard experiments have attracted enormous interest. In particular, we refer to Refs. [9,10] where ultracold atoms bounce off beams of light that form the boundary of the billiard. Experiments performed by Chinnery and Humphrey are worth noting since they provide a mesoscopic approach to the field that allows for excellent comparison between experiment or numerics and theory. They investigated acoustic resonances of an insonified water-filled stadium billiard with a schlieren visualizing system [11]. Moreover, much effort has been devoted to classical, semiclassical, and quantum mechanical studies on regularity and chaos in billiards [12–21].

Billiards whose walls are not fully reflective, or completely closed, play an important role as models to study chaotic phenomena in open systems but also have a vast bulk of applications, e.g., in the field of optical microresonators

where chaoticity is desired to significantly enhance the emission directionality [22]. Stadium-shaped microcavities have been studied in a number of publications [23]. For several geometries the dynamics of billiards with a single hole in the boundary have been investigated in the context of the decay of chaotic systems and chaotic wave scattering [24–26]. In order to demonstrate the existence of Maxwell’s daemon in chaotic billiards, Zaslavsky coupled two billiards through a small hole [27]. Interestingly, the daemon accomplishes a difference in the pressures of the two chaotic particle gases. A beautiful example for a two-hole leaking of the circle billiard represents Bunimovich and Dettmann’s demonstration of a direct connection between leaking billiard experiments and the Riemann hypothesis [28]. We also mention works on chaotic scattering in ballistic circle and stadium microstructures, cross junctions, and cut-circle billiards [29–33]. Electric density measurements of leaking microwave billiards in configuration space have been performed by Alt and co-workers [34,35].

Besides billiards, *leaking Hamiltonian systems* have been studied in different contexts, e.g., for the standard map, the restricted three-body problem of celestial mechanics, and transport problems in incompressible fluids [36,37]. It has been shown that suitable Poincaré surface of sections where

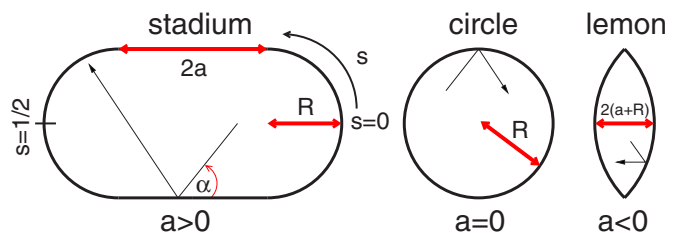


FIG. 1. (Color online) Schematic representation of stadium ($a > 0$), circle ($a=0$), and lemon-shaped ($a < 0$) billiard.

points are colored with respect to the corresponding orbit's escape time reveal computationally quickly a backbone of the system's phase-space and provide considerable insight in the leaking dynamics of the system. In the next sections we apply this approach to the stadium-lemon-billiard family, see Fig. 1. Instead of opening the boundary we introduce a small leakage inside the billiard. An experimental realization could be a microwave billiard where the antenna plays the role of the internal leakage [34,35].

II. MODEL

Bunimovich first considered a stadium billiard where two semicircular arcs with radii R are joined by tangential straight lines with lengths $2a > 0$ [38], see Fig. 1. The limiting case $a=0$ is the integrable circle billiard. Recent interest has been devoted to the case $-2 < a < 0$ where straight lines no longer exist but two circular sectors form a boundary which resembles a lense or lemon [14,17].

The phase-space of this one-parameter family of billiards is conveniently described by Birkhoff's coordinates: the (normalized) arc-length coordinate $0 \leq s < 1$ along the boundary and $p \equiv \cos(\alpha)$ being the momentum coordinate (energy is scaled out) where $0 < \alpha < \pi$ is the incident angle. With this choice of coordinates the phase-space mapping $\mathcal{M}: (s_n, p_n) \rightarrow (s_{n+1}, p_{n+1})$ is symplectic [12]. The radii R in Fig. 1 can be scaled out and the cases $p = \pm 1$ correspond to orbits being tangential to the boundary. Hence throughout the paper we assume unit system radii $R \equiv 1$ and consider the phase-space specified by $0 \leq s < 1$, and $-1 < p < 1$.

For the nontrivial cases $a \neq 0$, there are two reflexion symmetries that can be expressed by the operation $\mathcal{S}: (s, p) \rightarrow f(s, p)$ where

$$f(s, p) = \begin{cases} (s, p) & \text{for } 0 \leq s < 1/4, \\ (1/2 - s, -p) & \text{for } 1/4 \leq s < 1/2, \\ (s - 1/2, p) & \text{for } 1/2 \leq s < 3/4, \\ (1 - s, -p) & \text{for } 3/4 \leq s < 1. \end{cases} \quad (1)$$

Note that due to the arclength normalization, \mathcal{S} is independent of geometry parameter a . In addition to the reflexion symmetries, the billiard exhibits a time-reversal symmetry $\mathcal{T}: (s, p) \rightarrow (s, -p)$. It is important to mention that, first, throughout the paper we partly break the symmetries by placing a leakage inside the billiard, and second, the leakage can be formally considered an internal boundary.

III. ESCAPE TIME DIAGRAMS

We now investigate position and extent of escape orbits for the case that a circular leakage with radius ϵ is placed in the configuration space. We consider different positions of the circular leakage as illustrated in Fig. 2.

Figure 3 shows an escape time diagram (ETD) for the (s, p) plane. Each point represents a starting point in phase-space. The color codes the number of reflections before escape.

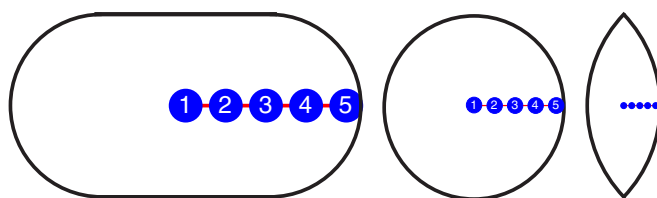


FIG. 2. (Color online) Schematic view of the leakage positions (disks). Half of the system size is portioned in such a way that five disks are placed equidistantly, disk 1 is centered, and disk 5 is tangent to the boundary.

A. Stadium billiard

Figure 4 displays the ETDs for the stadium billiards. The white horizontal stripes in the ETDs represent the (marginally stable) orbits created by perpendicular reflections between the stadiums' straight line segments. These orbits are called bouncing-ball orbits. The dimension of the leakage is imprinted in the diagrams: The width of the *slits* in the upper ETDs represents the hole diameter 2ϵ . The stripe-shaped regions in black represent particles that leak out after a single reflection. The upper diagram line corresponds to billiards that are leaked by circular middle holes of radii $\epsilon=0.01$, $\epsilon=0.05$, $\epsilon=0.1$, and $\epsilon=0.2$. If the circular leakages are replaced by quadratic leakages of equal areas, corresponding (magnifications of the) ETDs are virtually unaffected (not shown). As illustrated in the lower diagram line in Fig. 4 the position of the leakage (see Fig. 2) has a widely more profound impact on the diagram structure than the leakage geometry. Note that shifting the hole away from the center of the billiard breaks one of the reflexion symmetries.

Figure 5 shows the dependence of the escape time diagrams on the control parameter a for the stadium case $a > 0$. Though the phase-space is known to be hyperbolic for any $a > 0$, the escape time diagrams demonstrate the exist-

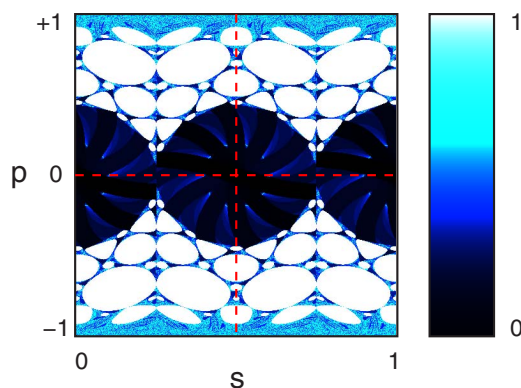


FIG. 3. (Color online) Ranges and color legend for escape time diagrams (ETD). Parameter values for the displayed example with central circular hole: $a = -0.2$, hole radius $\epsilon = 0.05$, and $N_{\max} = 10\,000$. The color legend displays the normalized escape time n_{esc}/N_{\max} where n_{esc} is the number of reflections before escape, and N_{\max} denotes the maximal number of reflections during the simulation. The lighter the color the longer the particle is trapped in the billiard. White colored phase-space points correspond to $n_{\text{esc}} = N_{\max}$, black ones correspond to $n_{\text{esc}} = 1$.

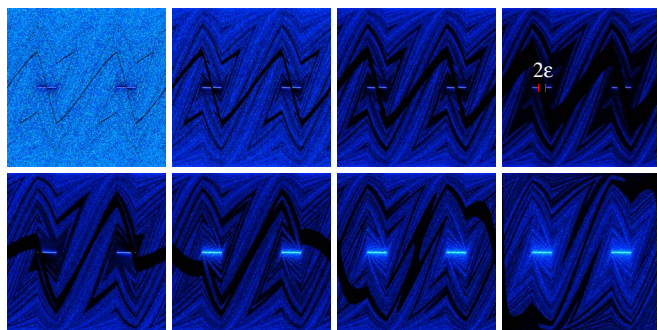


FIG. 4. (Color online) Escape time diagrams for the Birkhoff phase space, i.e., the (s, p) plane, and for $a=1$. The color of a point codes the number of reflections before escape through a circular central leakage (upper diagram line), and decentrally placed leakages (lower line). White points represent bounded motion (maximal number of specular reflection is $N_{\max}=10\,000$), all other points represent starting positions of escape orbits. The lighter the color, the larger the number of reflections (see scale in Fig. 3): black ($n_{\text{esc}}=1$), white ($n_{\text{esc}}=N_{\max}$). Upper line, from left to right: hole radius $\epsilon=0.01$, $\epsilon=0.05$, $\epsilon=0.1$, and $\epsilon=0.2$. Lower line: decentral disk positions 2, 3, 4, and 5 (see Fig. 2) for fixed radius $\epsilon=0.1$.

tence of a rather complex topology on position and extent of long- and short-lived motion. Figure 5 displays the situation for eight different values of a . First, the regular phase-space for $a=0$ (see black stripe in Fig. 6) is more and more ragged with increasing parameter value a . Second, the dominance of long-lived motion of the circularlike geometries $a \approx 0$ is destroyed by the onset of escape regions. The inset in the ETD for $a=0.1$ in Fig. 5 displays the ETD when the leakage is placed tangential to the boundary (see Fig. 2, position 5)—rather than central. As a consequence, even for values of a close to zero, regions of long-lived motion are displaced by regions of escape due to tangential leakage of the so-called *whispering-gallery* orbits with $p \approx \pm 1$.

B. Lemon billiard

We now investigate the mixed phase-space domain of the stadium-lemon-billiard family, that is, the parameter region

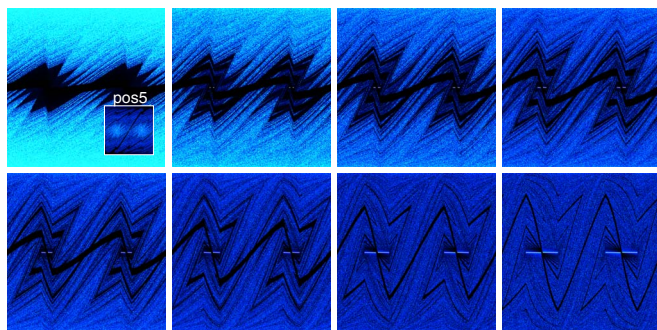


FIG. 5. (Color online) Escape time diagrams for the stadium billiard with central circular hole of radius $\epsilon=0.05$ for varying values of $a > 0$. Values for a from left to right: 0.1, 0.2, 0.3, 0.4 (upper diagram line), 0.5, 0.8, 1.4, 2.1 (lower diagram line). Inset: ETD for $a=0.1$ but for the tangential leakage position 5.

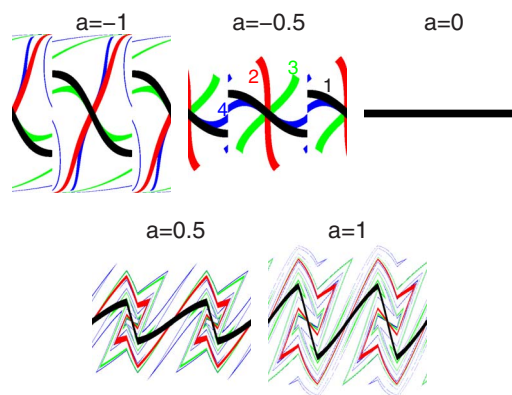


FIG. 6. (Color online) Iteration maps for lemon-shaped ($a=-1.0$, $a=-0.5$), circle ($a=0$), and stadium ($a=0.5$, $a=1.0$) billiard for a centered (position 1 in Fig. 2) circular leakage with radius $\epsilon=0.05$. The diagram plane is the (full) phase-space region ($0 < s \leq 1$, $-1 < p < 1$) (see also Fig. 3). Black points indicate an escape after a single reflection when the trajectory begins at the corresponding starting position in phase-space (s, p) . Red points represent trajectories which end up in the hole after two reflections, green and blue correspond to three and four reflections, respectively. White indicates a survival after four reflections.

$a < 0$. In Fig. 7 we provide a phase-space overview displaying ETDs for the range $-2 < a < 0$. The phase-space structure of each diagram is partitioned into three main domains. White colored island chains of regular (almost quasiperiodic) motion with the corresponding periodic centers (not shown) in a *sea* of highly structured chaos (light or blue regions). The linear scale of the leakage is represented in the plain unstructured (nonfractal) *escape basins* in black or dark blue. The insets in the ETD for $a=-0.1$ in Fig. 7 show the behavior for $a \rightarrow -0$. For examples of corresponding orbits (that are not hindered by the leakage) we refer to the bulk of literature triggered by the coining paper, Ref. [14].

We now investigate how the position of the leakage affects the phase-space structure in the ETDs for $a < 0$. In Fig. 8 we show for five different values of the geometry parameter a four diagrams corresponding to four off-centered leakage positions. More precisely, each diagram line provides the ETDs for the leakage positions 2, 3, 4, and 5 as explained in Fig. 2.

Under the shift of the leakage from the center to the border, islands representing never escaping orbits (partly) disappear when their corresponding quasiperiodic orbits are (partly) blocked by the leakage in configuration space, see the lower diagram line (e) in Fig. 8. In contrast to that behavior, lemon billiards with phase-space that is dominated by chaotic motion are not profoundly affected by the leakage position, see diagram line (b) corresponding to $a=-1$ in Fig. 8.

IV. MEAN ESCAPE TIME DISTRIBUTIONS

For billiards the (mean) escape time distribution has been studied both experimentally and theoretically, see in addition to the previously cited works, Ref. [39] and references therein. To be precise, we define the mean escape time as

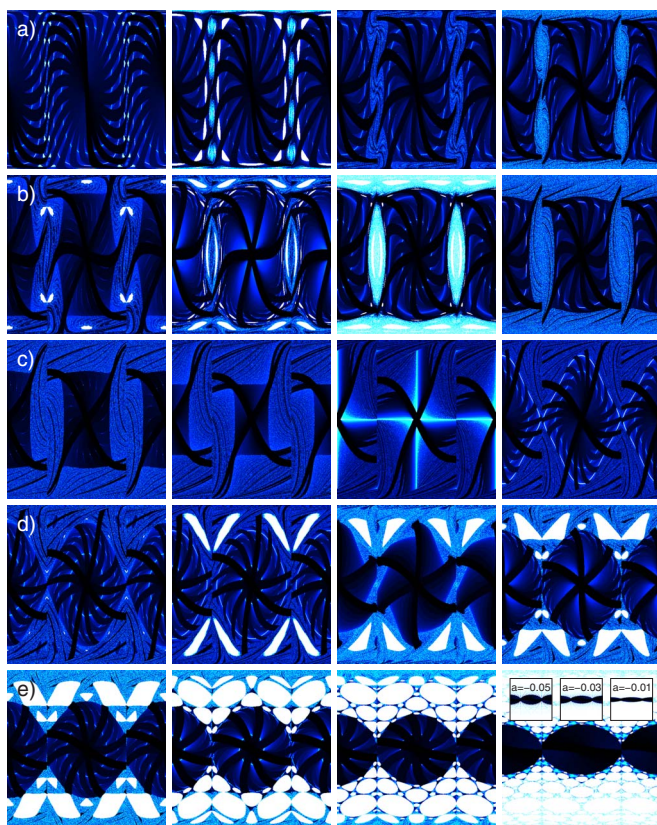


FIG. 7. (Color online) Escape time diagrams for various parameter values $a < 0$ for fixed circular hole radius, $\epsilon = 0.05$, that is centered. $N_{\max} = 10\,000$. Left to right: $-1.97, -1.9, -1.8, -1.7$ (a), $-1.6, -1.5, -1.4, -1.3$ (b), $-1.2, -1.1, -1.0, -0.9$ (c), $-0.8, -0.7, -0.6, -0.5$ (d), $-0.4, -0.3, -0.2, -0.1$ (e). Insets: ETD for $a = -0.05$, -0.03 , and $a = -0.01$.

$$\langle n_{\text{esc}} \rangle \equiv \langle n_{\text{esc}}(s, p) \rangle / N_{\max}, \quad (2)$$

where brackets $\langle \cdot \rangle$ on the right hand side denote the average over the phase-space ($0 \leq s < 1, -1 < p < 1$) and $n_{\text{esc}}(s, p)$ is the escape time (number of reflections) for each starting phase-space position (s, p) of the trajectory. As throughout the paper, N_{\max} is the maximal number of reflections.

A. Phase-space dominated by chaotic motion

In Fig. 9 we plot the mean escape time vs the leakage size for five different hole positions. As expected, for the hyperbolic cases $a = 0.5$ and $a = 1$ all curves are close to a power-law behavior. The power-law approximation of the decay is better the smaller the hole size: in Fig. 10 we plot the scaled mean escape time for $a = 1$ vs the hole radius for small values of the leakage size $10^{-4} \leq \epsilon < 10^{-1}$. As can be seen in the log-log-plot, for small leakage sizes, the mean escape time decays as a power of -1 . For large hole sizes, that is, of the order of the system size, finite-size effects cause deviations from the theoretical curve.

In the following we show that it is sufficient to consider the billiard map with strongly chaotic dynamics as a stochastic map in order to explain the power law for the mean escape time dependence on the leakage dimension. Let $P(n)$

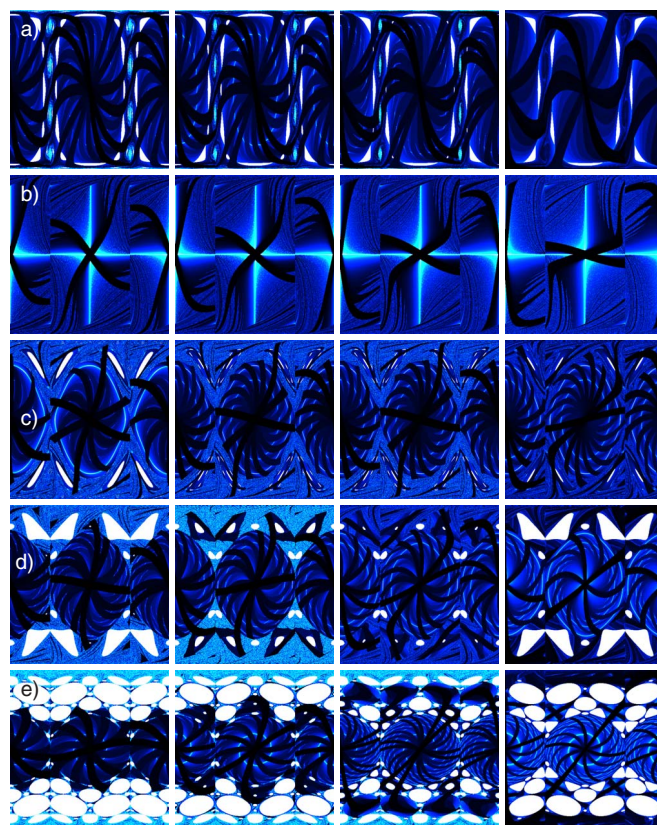


FIG. 8. (Color online) Escape time diagrams for four decentral positions of a circular hole. $\epsilon = 0.05$ is fixed, $N = 10\,000$. Left to right in a diagram line: leakage position 2, 3, 4, and 5. $a = -1.9$ (a), $a = -1.0$ (b), $a = -0.7$ (c), $a = -0.5$ (d), $a = -0.2$ (e).

denote the probability that the particle leaves the system after n elastic reflections. Denoting with p the probability to leave the system in a time step, the survival probability is then given by

$$P_{\text{surv}}(n) = (1 - p)^n \approx e^{-pn}. \quad (3)$$

The probability for the particle not to leave the system through the leakage during the first $n - 1$ reflections, but at

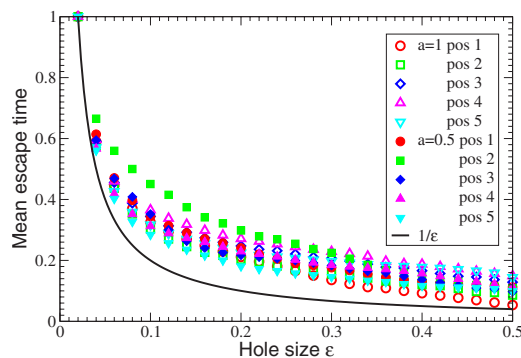


FIG. 9. (Color online) Mean escape time distribution dependence on circular leakage position for $a = 0.5$ (solid symbols), and for $a = 1$ (open symbols). The bold line is the power law $1/\epsilon$. Curves are arbitrarily normalized to coincide at $\langle n_{\text{esc}} \rangle = 1$.

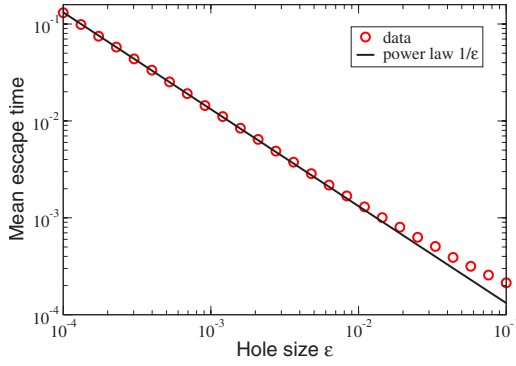


FIG. 10. (Color online) Mean escape time distribution for small circular leakages in a double-logarithmic plot ($a=1.0$). For small leakage sizes data are in good agreement with the theoretical curve (power law).

time step n , is given by $P(n) = P_{\text{surv}}(n-1) \times p$. Putting this together we have

$$\begin{aligned}
 \langle n_{\text{esc}} \rangle &= \sum_{n=1}^{\infty} n P(n) \\
 &= \frac{p}{1-p} \sum_{n=1}^{\infty} n (1-p)^n \\
 &= \frac{p}{1-p} \left[q \frac{d}{dq} \sum_{n=0}^{\infty} q^n \right]_{q=1-p} \\
 &= \frac{p}{1-p} \left[\frac{q}{(1-q)^2} \right]_{q=1-p} \\
 &= \frac{1}{p}, \tag{4}
 \end{aligned}$$

where we here consider the limit $N_{\text{max}} \rightarrow \infty$. Since the hole represents a stripe in phase-space, the escape probability in each time step is $p = \epsilon/A$, A being the total area in phase-space. Hence we obtain $\langle n_{\text{esc}} \rangle \sim \epsilon^{-1}$ in good agreement with the data for $\epsilon \ll 1$.

B. Phase-space dominated by regular motion

Figure 11 shows the mean escape distribution for the quasiregular case $a=0.1$. We mean by quasiregular the case when the Lyapunov exponent of a hyperbolic system is positive but close to zero (as for $a \rightarrow 0$). As a consequence, the ETDs are dominated by quasiregular orbits (see, e.g., light or blue regions in Fig. 5). In contrast to Fig. 9, only for the tangential leakage position can the mean escape distribution be approximated by the $1/\epsilon$ power law. We can understand this behavior because for the billiard with the tangential leakage *whispering-gallery* orbits can leave the system (see also inset in Fig. 5). All other data curves corresponding to positions 1–4 (see Fig. 2) lie between the $1/\epsilon$ law and a $1-\epsilon$ curve, the origin of which will be explained later.

In Fig. 12 we plot the mean escape times of billiard systems whose distributions can be well approximated by either theoretical curve. Strikingly, systems dominated by regular

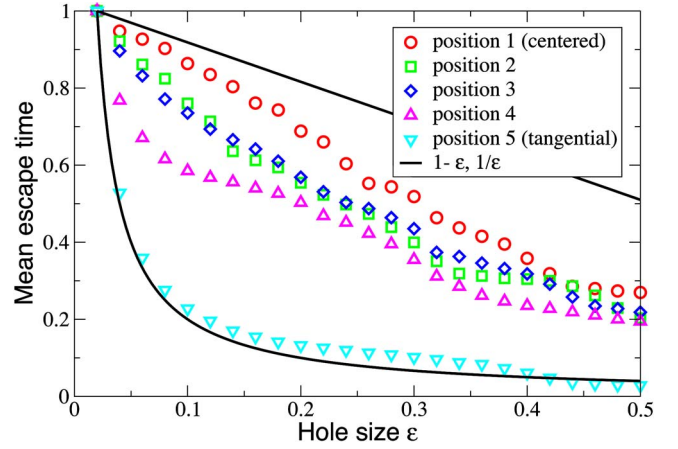


FIG. 11. (Color online) Mean escape time distribution for $a=0.1$ and five leakage positions. The bold lines are the theoretical curves $1-\epsilon$ and $1/\epsilon$, respectively. Curves are arbitrarily normalized to coincide at $\langle n_{\text{esc}} \rangle = 1$.

motion have distributions that follow the $1-\epsilon$ law, and systems with phase-space dominated by chaotic motion have distributions that can be well approximated by the $1/\epsilon$ law. Note that in contrast to the survival probability function $P_{\text{surv}}(t)$ measurements in the literature for different mixed chaotic systems [39], $P(\epsilon)$ cannot be approximated by simple crossovers of power laws or exponential decays. The *fine structure* of the $P(\epsilon)$ curves for the mixed phase-space mirrors the dependence on position and extent of resonances, and leakage position.

If the phase-space is dominated by regular regions, leaking the phase-space has the effect that the regular regions in the Poincaré surface of section are *flooded* by regions of escape. For the integrable circle billiard, being the case $a=0$, this fact is straightforward to see. Consider a hole in the unit circle billiard centered in the middle, with radius $\epsilon < 1$. Trajectories that have a tangential intersection with the hole must satisfy

$$|\cos(\alpha)| = \epsilon, \tag{5}$$

if α denotes the incident angle, see Fig. 1. Due to the identity $p \equiv \cos(\alpha)$, for every starting position s on the unit circle,

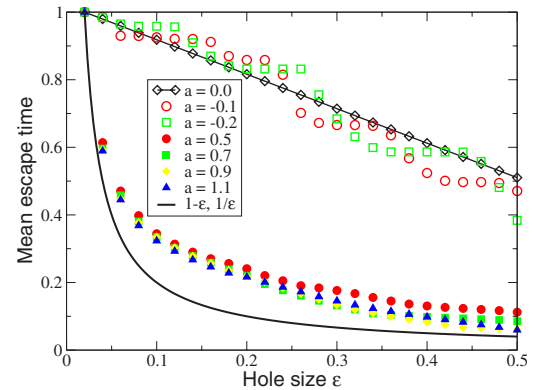


FIG. 12. (Color online) Mean escape time distribution. Average escape time vs linear hole size. The bold lines are the theoretical curves $1-\epsilon$ and $1/\epsilon$, respectively. Curves are arbitrarily normalized to coincide at $\langle n_{\text{esc}} \rangle = 1$.

trajectories with momentum $-\epsilon \leq p \leq \epsilon$ will escape through the leakage. As a consequence, the fraction of escape orbits A_{esc} in the (s, p) plane, $0 \leq s < 1$, $-1 < p < 1$, is $A_{\text{esc}} = \frac{2 \times \epsilon}{2} = \epsilon$ from which we read off the mean escape time (in the limit $N_{\text{max}} \rightarrow \infty$) as $\langle n_{\text{esc}} \rangle = 1 - \epsilon$.

V. CONCLUSIONS

We studied the dynamics of leaking billiards. Rather than open the boundary we considered leakages inside the billiard. Our investigation was motivated by works on leaking Hamiltonian systems together with recent applications. As a suitable one-parameter billiard system we focused on the stadium-lemon-billiard family as a prominent chaotic system that can be tuned from fully hyperbolic behavior to a mixed chaotic behavior. In the context of *leaking* Hamiltonian systems [37], it is known that leaking is capable to reveal the phase-space structure (i.e., the chaotic saddle), here represented in terms of escape time diagrams. We demonstrated how the position and geometry of the leakage affects the

dynamics. The mean escape time dependence on the size of the leakage is algebraic—as known for openings of the boundary for hyperbolic systems [24]. This finding corresponds to an exponentially decaying survival probability distribution and could be fully explained by a stochastic map approach. On the other hand, for systems where the phase-space consists to a large extent of regular orbits, we numerically found a linear dependence of the mean escape time on the leakage dimension as $\langle n_{\text{esc}} \rangle \sim 1 - \epsilon$. Regions of regular orbits in phase-space are *flooded* by escape domains as the leakage increases. For the integrable circle billiard we comprehended the phenomenon analytically.

In a slightly broader context, our investigations extend recent work on time continuous leaking systems [36] and represent examples for leaking Hamiltonian systems in their configuration space.

ACKNOWLEDGMENT

We gratefully acknowledge Peter H. Richter for helpful comments and for the careful reading of the manuscript.

-
- [1] G. Benettin, *Physica D* **13D**, 211 (1984).
 [2] H. Makino, T. Harayama, and Y. Aizawa, *Phys. Rev. E* **63**, 056203 (2001).
 [3] J. A. Katine, M. A. Eriksson, A. S. Adourian, R. M. Westervelt, J. D. Edwards, A. Lupu-Sax, E. J. Heller, K. L. Campman, and A. C. Gossard, *Phys. Rev. Lett.* **79**, 4806 (1997).
 [4] H.-J. Stöckmann and J. Stein, *Phys. Rev. Lett.* **64**, 2215 (1990).
 [5] B. Dietz, A. Heine, A. Richter, O. Bohigas, and P. Leboeuf, *Phys. Rev. E* **73**, 035201(R) (2006).
 [6] S. Sridhar and E. J. Heller, *Phys. Rev. A* **46**, R1728 (1992).
 [7] H.-S. Sim and H. Schomerus, *Phys. Rev. Lett.* **89**, 066801 (2002).
 [8] H.-J. Stöckmann, *Quantum Chaos: An Introduction* (Cambridge University Press, New York, 1999).
 [9] N. Friedman, A. Kaplan, D. Carasso, and N. Davidson, *Phys. Rev. Lett.* **86**, 1518 (2001).
 [10] V. Milner, J. L. Hanssen, W. C. Campbell, and M. G. Raizen, *Phys. Rev. Lett.* **86**, 1514 (2001).
 [11] P. A. Chinnery and V. F. Humphrey, *Phys. Rev. E* **53**, 272 (1996).
 [12] M. V. Berry, *Eur. J. Phys.* **2**, 91 (1981).
 [13] O. Biham and M. Kvale, *Phys. Rev. A* **46**, 6334 (1992).
 [14] E. J. Heller and S. Tomsovic, *Phys. Today* **46**(7), 38 (1993).
 [15] S. Tomsovic and E. J. Heller, *Phys. Rev. E* **47**, 282 (1993).
 [16] P. H. Richter, H.-J. Scholz, and A. Wittek, *Nonlinearity* **3**, 45 (1990).
 [17] H. R. Dullin, P. H. Richter, and A. Wittek, *Chaos* **6**, 43 (1996).
 [18] H. Waalkens, J. Wiersig, and H. R. Dullin, *Ann. Phys. (N.Y.)* **260**, 50 (1997).
 [19] S. Ree and L. E. Reichl, *Phys. Rev. E* **60**, 1607 (1999).
 [20] V. Lopac, I. Mrkonjić, and D. Radić, *Phys. Rev. E* **59**, 303 (1999); **66**, 036202 (2002).
 [21] J. Wiersig, *Phys. Rev. E* **62**, R21 (2000); **64**, 026212 (2001).
 [22] Jens U. Nöckel and A. Douglas Stone, *Nature (London)* **385**, 45 (1997); C. Gmachl, F. Capasso, E. E. Narimanov, J. U. Nöckel, A. D. Stone, J. Faist, D. L. Sivco, and A. Y. Cho, *Science* **280**, 1556 (1998); T. Ben-Messaoud and J. Zyss, *Appl. Phys. Lett.* **86**, 241110 (2005); J. Wiersig and M. Hentschel, *Phys. Rev. A* **73**, 031802(R) (2006).
 [23] T. Harayama, P. Davis, and K. S. Ikeda, *Phys. Rev. Lett.* **90**, 063901 (2003); T. Harayama, T. Fukushima, S. Sunada, and K. S. Ikeda, *ibid.* **91**, 073903 (2003); T. Fukushima and T. Harayama, *IEEE J. Sel. Top. Quantum Electron.* **10**, 1039 (2004); T. Fukushima, T. Harayama, and J. Wiersig, *Phys. Rev. A* **73**, 023816(R) (2006).
 [24] H. Alt, H.-D. Gräf, H. L. Harney, R. Hofferbert, H. Rehfeld, A. Richter, and P. Schardt, *Phys. Rev. E* **53**, 2217 (1996).
 [25] W. Bauer and G. F. Bertsch, *Phys. Rev. Lett.* **65**, 2213 (1990); O. Legrand and D. Sornette, *ibid.* **66**, 2172 (1991); W. Bauer and G. F. Bertsch, *ibid.* **66**, 2173 (1991); O. Legrand and D. Sornette, *Physica D* **44**, 229 (1990).
 [26] E. Doron, U. Smilansky, and A. Frenkel, *Phys. Rev. Lett.* **65**, 3072 (1990).
 [27] G. M. Zaslavsky, *Phys. Today* **52**(8), 39 (1999).
 [28] L. A. Bunimovich and C. P. Dettmann, *Phys. Rev. Lett.* **94**, 100201 (2005).
 [29] S. Ree and L. E. Reichl, *Phys. Rev. E* **65**, 055205(R) (2002).
 [30] R. A. Jalabert, H. U. Baranger, and A. D. Stone, *Phys. Rev. Lett.* **65**, 2442 (1990).
 [31] M. L. Roukes and O. L. Alerhand, *Phys. Rev. Lett.* **65**, 1651 (1990).
 [32] P. Jacquod, *Phys. Rev. E* **72**, 056203 (2005).
 [33] C. M. Marcus, A. J. Rimberg, R. M. Westervelt, P. F. Hopkins, and A. C. Gossard, *Phys. Rev. Lett.* **69**, 506 (1992).
 [34] H. Alt, C. I. Barbosa, H.-D. Gräf, T. Guhr, H. L. Harney, R. Hofferbert, H. Rehfeld, and A. Richter, *Phys. Rev. Lett.* **81**, 4847 (1998).

- [35] H. Alt, C. Dembowski, H.-D. Gräf, R. Hofferbert, H. Rehfeld, A. Richter, and C. Schmit, *Phys. Rev. E* **60**, 2851 (1999).
- [36] J. Nagler, *Phys. Rev. E* **69**, 066218 (2004); **71**, 026227 (2005).
- [37] J. Schneider, Tamás Tél, and Zoltán Neufeld, *Phys. Rev. E* **66**, 066218 (2002); I. Tuval, J. Schneider, O. Piro, and T. Tél, *Europhys. Lett.* **65**, 633 (2004).
- [38] L. A. Bunimovich, *Funct. Anal. Appl.* **8**, 254 (1974); *Commun. Math. Phys.* **65**, 295 (1979).
- [39] A. J. Fendrik, A. M. F. Rivas, and M. J. Sánchez, *Phys. Rev. E* **50**, 1948 (1994); Y.-C. Lai, M. Ding, C. Grebogi, and R. Blümel, *Phys. Rev. A* **46**, 4661 (1992).